GEOPHYSICS, VOL. 62, NO. 4 (JULY-AUGUST 1997); P. 1151–1162, 9 FIGS.

Effects of pore structure and wettability on the electrical resistivity of partially saturated rocks—A network study

Ravi J. Suman* and Rosemary J. Knight‡

ABSTRACT

A network model of porous media is used to assess the effects of pore structure and matrix wettability on the resistivity of partially saturated rocks. Our focus is the magnitude of the saturation exponent n from Archie's law and the hysteresis in resistivity between drainage and imbibition cycles.

Wettability is found to have the dominant effect on resistivity. The network model is used to investigate the role of a wetting film in water-wet systems, and the behavior of oil-wet systems. In the presence of a thin wetting film in water-wet systems, the observed variation in n with saturation is reduced significantly resulting in lower n values and reduced hysteresis. This is attributed to the electrical continuity provided by the film at low-water saturation between otherwise physically isolated portions of water. Oil-wet systems, when compared with the water-wet systems, are found to have higher n values. In addition, the oil-wet systems exhibit a different form of hysteresis and more pronounced hysteresis. These differences in the resistivity response are attributed to differences in the pore scale distribution of water.

The effects of pore structure are assessed by varying pore size distribution and standard deviation of the pore size distribution and considering networks with pore size correlation. The most significant parameter is found to be the pore size correlation. When the sizes of the neighboring pores of the network are correlated positively, the magnitude of n and hysteresis are reduced substantially in both the water-wet and oil-wet systems. This is attributed to higher pore accessibility in the correlated networks.

The results of the present study emphasize the importance of conducting laboratory measurements on core samples with reservoir fluids and wettability that is representative of the reservoir. Hysteresis in resistivity can be present, particularly in oil-wet systems, and should be considered in the interpretation of resistivity data.

INTRODUCTION

Electrical resistivity measurements are used commonly to estimate in-situ water saturation in hydrocarbon reservoirs. The interpretation of these measurements is usually based on Archie's law (Archie, 1942), which relates the resistivity index I of a partially saturated rock to the level of water saturation S_w according to

$$I = S_w^{-n}.$$

The resistivity index, $I = R_t/R_0$, where R_t and R_0 are the resistivities of the partially and fully water-saturated rock, respectively, and n is the saturation exponent. For an estimation of in-situ water saturation, R_t and R_0 are obtained from well logs, whereas n is found from laboratory measurements on reservoir cores.

Implicit to the above approach are the assumptions that: (1) the resistivity index-water saturation relationship for a given porous medium can be characterized by a constant and unique n, and (2) the n values determined in the laboratory are applicable to the reservoir. A number of laboratory studies have shown, however, that under many situations these assumptions may not be valid. For example, for the same sample, n can be a function of water saturation and saturation history. Also, the laboratory derived n values may not be representative of the

Manuscript received by the Editor August 11, 1995; revised manuscript received September 4, 1996.
*Formerly Department of Geophysics and Astronomy, The University of British Columbia, 2219 Main Mall, Vancouver, BC V6T 1Z4, Canada; presently AGAT Laboratories, A 3700, 21 St. N.E., Calgary AB T2E 6V6 Canada.
‡Department of Geophysics and Astronomy, The University of British Columbia, 2219 Main Mall, Vancouver, BC V6T 1Z4, Canada. E-mail:knight@geop.ubc.ca.
© 1997 Society of Exploration Geophysicists. All rights reserved.

reservoir conditions if the wettability of the laboratory samples differs from that of the reservoir.

A number of factors can affect the resistivity response of rocks. Of specific interest in this study are pore structure and matrix wettability, both of which influence resistivity through their control on pore-scale fluid distributions. The role of pore structure in the electrical behavior of rocks has not been investigated experimentally because of the prohibitively large number of variables involved in such studies. However, a number of recent theoretical investigations (e.g., Chatzis and Dullien, 1985; Wardlaw et al., 1987; Tsakiroglou and Payatakes, 1991) have indicated a significant effect of pore size correlations on capillary pressure curves, suggesting that this aspect of pore structure may also be important in determining the electrical response of a rock. The role of wettability has been the focus of numerous experimental investigations over the last four decades. Wettability has been found to strongly affect the magnitude of n and the hysteresis in n between drainage and imbibition cycles. The n values are found to be higher significantly in oil-wet systems than in water-wet systems (e.g., Keller, 1953; Rust, 1957; Sweeney and Jennings, 1960; Morgan and Pirson, 1964; Mungan and Moore, 1968; Donaldson and Bizerra, 1985; Lewis, 1988; and Donaldson and Siddiqui, 1989). The hysteresis in water-wet systems is found to be either absent (e.g., Mungan and Moore, 1968; Sanyal and Ramey, 1973) or very small (e.g., Swanson, 1980; Longeron et al., 1989; Sharma et al., 1991). In contrast, the hysteresis in oil-wet systems is found to be considerably higher (Wei and Lile, 1991; Sharma et al., 1991).

Pore structure and wettability can vary greatly within a reservoir and from reservoir to reservoir. Therefore, a thorough understanding of the effects of these parameters on the resistivity response is essential for an accurate prediction of in-situ water saturation from resistivity measurements. We have conducted a systematic and detailed study to assess the effects of pore structure and wettability on the resistivity response of partially saturated rocks using a pore network model of porous media.

Network models have proven to be invaluable tools for investigating the effects of pore-level phenomena on the bulk properties of porous media. These models have a unique advantage in that they can be employed to isolate the effects associated with different parameters. This is difficult to accomplish in the laboratory investigations because of the large number of variables involved. A typical porous medium consists of intersecting channels of varying sizes. The channels have a very small open flow area and therefore the average fluid flow and transport of electric charge through the fluid inside a channel are essentially in the direction of its axis. A cylindrical tube-shaped pore, which is the basic element of the present network, adequately captures this feature. The network also incorporates features such as the size distribution of channels and channel intersections and thus is a valid representation of porous media for studying the resistivity response of partially saturated rocks.

In his pioneering work, Fatt (1956) was the first to conclude that the pore networks were valid models of real porous media and that the resistivity curves for networks were qualitatively similar to those for real porous media. Since then, network models have been used by Greenberg and Brace (1969), Shankland and Waff (1974), and Wang and Sharma (1988) to investigate the resistivity response of rocks. In the most recent of these studies, Wang and Sharma (1988) demonstrated several important effects of pore structure and wettability on the I-S_w relationship. However, their approach is limited to symmetrical pore size distributions and uses the same pore accessibility function during both drainage and imbibition cycles.

In this study, we employ a 3-D network model of porous media to study the effects of pore structure features and wettability on the I-S_w relationship of partially saturated rocks. Of specific interest to this study is the magnitude of the saturation exponent n and the form and magnitude of hysteresis in resistivity between drainage and imbibition cycles. We study the effects of pore size distribution, standard deviation of pore size distribution, and positive correlation between the sizes of the neighboring pores. The effects of wettability are studied by comparing the results of the water-wet and oil-wet systems. As a special case of water-wet systems, we also investigate the effects of a thin water film coating the solid surface.

FEATURES OF THE NETWORK MODEL

Figure 1 shows the schematic of the 3-D cubic pore network model considered in this study. The bonds in the network represent the circular cylindrical pores that may be straight or tortuous. The points where the pores meet are called the junctions. The pores at a junction are assumed to meet in such a manner as to not create any additional pore volume other than that represented by the pores themselves. The network consists of γ tiers, where each tier has α columns and β rows of junctions. Six pores meet at a junction, therefore the coordination number of the model is 6.

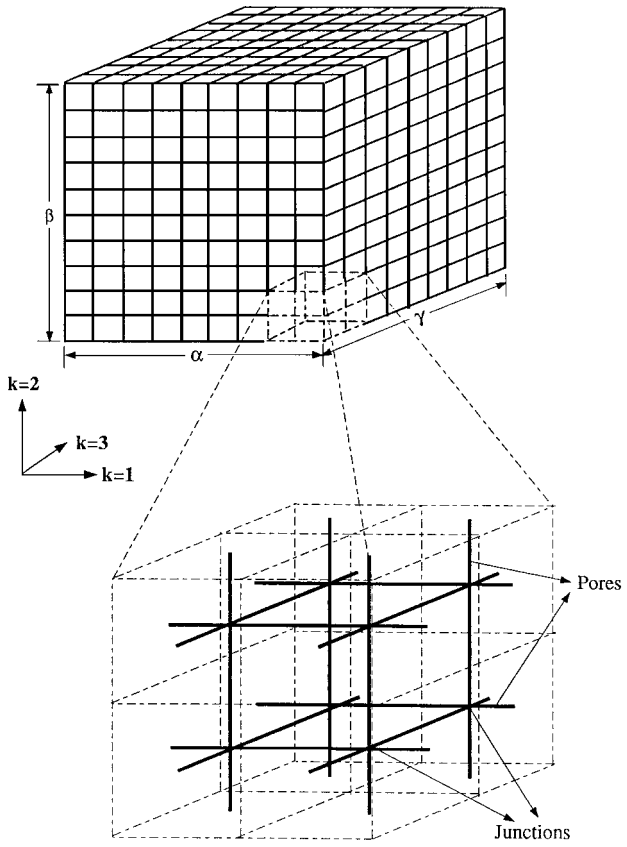

FIG. 1. Schematic showing different features of the 3-D cubic network with α columns, β rows and γ tiers of junctions. The $k = 1$, 2, and 3 represent the three principal directions.

As shown in Figure 1, the $k = 1, 2, 3$ represents the three principal directions. The $k = 1$ is the bulk flow direction. The face normal to the $k = -1$ direction is the upstream side and the face normal to the $k = 1$ direction is the downstream side. The remaining four faces of the network are sealed, that is, no flow is allowed across these faces.

In principle, an infinite number of parameters is required to completely characterize the pore structure of a natural porous medium. By considering idealized models, this number is reduced significantly. The present model is characterized completely by five pore structure parameters—the pore diameter distribution, mean pore diameter, standard deviation of pore diameter distribution, pore tortuosity, and pore density. We consider rectangular, normal, and lognormal pore diameter distributions. Since changing the mean pore diameter has the opposite effect of changing the standard deviation of the pore size distribution, we fix the mean pore diameter at 5.4 μm and only study the effects of standard deviation. In fact, it is the ratio of the standard deviation and mean, called the coefficient of variation, that is found to be relevant. The pore tortuosity is the mean of the ratio of the pore lengths and the corresponding bulk lengths of the network. We assign a fixed length to the pores with a resulting tortuosity of 1.1. As argued in Nicholson et al. (1988), this assumption is no more arbitrary than the one used in Fatt (1956) in which a relation was used between the diameter and length of a pore. The pore density is the ratio of the number of pores in a principal direction intersecting a plane normal to that direction and the bulk area normal to that direction. The pore density is a measure of the porosity of the network. Since the effects related to porosity are not of primary interest in this study, we fix the pore density in all the three principal directions at $2.4 \times 10^9/\text{m}^2$. This value of pore density results in porosities of 0.188, 0.195, and 0.206 for standard deviations of 1.0, 1.5, and 2.0 μm, respectively.

A $10 \times 10 \times 10$ ($\alpha = \beta = \gamma = 10$) network is used. To determine whether this was a sufficient size, a number of simulations were first run on a Fujitsu VPX240 supercomputer, with each simulation taking approximately 50 minutes. The results indicated that the $10 \times 10 \times 10$ network is sufficient for modeling capillary pressure curves and I-S_w relationships.

For generating pore size correlations, a modified version of the algorithm of Tsakiroglou and Payatakes (1991) is employed. First a given number of pore diameters equal to the number of pore locations are generated according to a given distribution. The diameters are then ranked and partitioned in a number of classes, each containing the same number of pore diameters. A diameter is randomly chosen from these classes as a "seed" and assigned to a random pore location in the network. The diameter is then removed from the class to which it belongs. This step is repeated for a small fraction of the total number of pore locations of the network. For each as yet unoccupied pore locations next to a seed pore, a diameter from the same class, J, as the seed pore, is chosen. If, during this procedure, class J becomes empty, then a diameter from the class $J-1$ or $J+1$ is chosen. If both of these classes are empty, the choice is made from the next class, $J-2$ or $J+2$, and so on. This procedure is carried out for each seed pore so that diameters are assigned to all immediate neighbors of the seed pores. Each of these newly assigned pore locations is treated from that point as a new seed pore, and the process is continued until diameters are assigned to all pore locations. This procedure results in a positive correlation between the sizes of the neighboring pores. In other words, pores of similar sizes cluster together inside the network.

To understand the role of wettability, we consider networks with three types of wettability characteristics. The first type are water-wet where wettability only dictates the pore scale fluid distribution. The second type are also water-wet but in addition have a thin water film coating the solid surface. The third type are oil-wet.

ALGORITHM FOR SIMULATING DRAINAGE AND IMBIBITION

The algorithm for drainage and imbibition is explained in terms of the wetting phase and nonwetting phase to generalize it for both the water-wet and oil-wet systems. For water-wet systems, water is the wetting phase and oil is the nonwetting phase whereas for oil-wet systems the opposite is the case. Water is the conducting phase in both the wettability systems. Drainage involves the displacement of the wetting phase by the nonwetting phase, whereas imbibition involves the displacement of the nonwetting phase by the wetting phase.

The drainage process is modeled by progressively replacing the wetting phase in the network with the nonwetting phase through an incremental increase in the nonwetting phase pressure. Initially, the network is visualized as being saturated completely by the wetting phase. A reservoir of the nonwetting phase is assumed to be on the upstream side and the wetting phase inside the network is assumed to be continuous with a wetting phase sink on the downstream side of the network. During the drainage process, only the wetting phase is allowed to leave the network through the downstream side and the nonwetting phase is confined to the network. This assumption is equivalent to the presence of a water-wet/oil-wet porous disk in the conventional methods for measuring two-phase capillary pressure curves. Piston type displacement is assumed inside the pores during both the drainage and imbibition and at any time only one phase is allowed to reside inside a pore.

To start the drainage process, pressure in the nonwetting phase reservoir is slowly increased (the wetting phase pressure is held constant) until the nonwetting phase starts to invade the network. At any given nonwetting phase pressure, the following three conditions must be met before the wetting phase inside a pore can be displaced by the nonwetting phase:

1) The prevailing difference between the nonwetting phase and wetting phase pressures, must be greater than or equal to the capillary pressure corresponding to the diameter of the pore;
2) the pore must be in contact with the nonwetting phase reservoir (directly or through the nonwetting phase in other pores); and
3) the wetting phase inside the pore must be in contact with the wetting phase sink (directly or through the wetting phase in other pores).

The wetting phase in the pores that is not continuous with the wetting phase sink becomes isolated and contributes to the irreducible wetting phase saturation. The freshly filled junctions at the ends of the invaded pores are stored as the potential displacement sites. All the pores connected to a filled junction that

satisfy the above three criteria are then invaded with the nonwetting phase. The process of filling the junctions and the pores is continued until the oil-water front is incapable of moving at the given capillary pressure. At this point, the water saturation and the resistivity index of the network are calculated. The nonwetting phase pressure is then raised in small increments and other points on the resistivity index curve are determined. The process is continued until irreducible wetting phase saturation is reached.

The imbibition process is initiated at the end of the drainage cycle by reducing the nonwetting phase pressure in small increments and allowing the wetting phase to imbibe back into the network. For the wetting phase to imbibe into a pore filled with the nonwetting phase, the following three conditions must be met:

1) The prevailing difference between the nonwetting phase and wetting phase pressure must be lower than the capillary pressure corresponding to the diameter of the pore;
2) the pore must be in contact with the wetting phase sink (directly or through other pores filled with the wetting phase); and
3) the nonwetting phase in the pore must be continuous with the nonwetting phase reservoir (directly or through other pores filled with the nonwetting phase).

The nonwetting phase that becomes isolated contributes to the residual nonwetting phase saturation. The process of imbibing the wetting phase into the junctions and pores is continued until the oil-water front is incapable of moving at the given capillary pressure. At this point the water saturation and resistivity index of the network are calculated. The procedure is repeated to find the other points on the resistivity index curve. The process is finally stopped when residual nonwetting phase saturation is reached.

To calculate the resistivity index of the network at a given water saturation, a potential drop is assumed across the network. The network is scanned to find all the pores and junctions that fall on continuous electrical paths from the upstream to the downstream side. Equations for current flow inside the electrically continuous pores are written in terms of the potentials at the junctions across the pores. Then Kirchhoff's current law is written for all the electrically continuous junctions. This results in as many simultaneous linear algebraic equations as there are electrically continuous junctions. The variables in these equations are the junction potentials. The set of simultaneous linear algebraic equations is inverted and junction potentials are determined. Once the junction potentials are known, the currents in the pores are calculated. The bulk current through the network is calculated by summing the currents in all the pores in the upstream or downstream face of the network. To calculate the resistivity index of the network at a given water saturation, the resistivity of the network is divided by the resistivity of the fully water-saturated network.

RESULTS AND DISCUSSION

We consider the effects of pore structure features and wettability on the magnitude of the saturation exponent n and the form and magnitude of the hysteresis in resistivity index between drainage and imbibition cycles. The pore structure features considered include pore size distribution, standard deviation of pore size distribution, and positive correlation between the sizes of the neighboring pores. The effects of wettability are studied by comparing the results of water-wet and oil-wet systems. As part of the assessment of wettability, we also consider the contribution of a thin wetting film to the overall electrical conduction in the water-wet systems.

To compare the resistivity behavior of different cases, we use two-point n values, which are based on the minimum and maximum observed values of resistivity index. Although use of two-point n values is not an exact method for characterizing the resistivity behavior of a system, it is useful for the purposes of comparison in this study.

Effects of pore structure

The mean pore diameter, pore tortuosity, and pore density for all the cases in this study are fixed at 5.4 μm, 1.1, and 2.4 $\times$ $10^9/m^2$, respectively.

Pore size distribution.—The effects of pore size distribution on resistivity are studied by considering water-wet networks with rectangular, normal, and lognormal pore size distributions. These results are illustrated in Figures 2a (rectangular), 2b (normal), and 2c (lognormal), which show log-log plots of resistivity index versus water saturation during drainage and imbibition. For all the three cases, the pore size distribution has a standard deviation of 1 μm.

The two-point n values for the three distributions are: 2.75 and 2.71 during drainage and imbibition for the rectangular distribution, 2.47 and 2.44 during drainage and imbibition for the normal distribution, and 2.70 and 2.73 during drainage and imbibition for the lognormal distribution. These n values and the shapes of the resistivity plots for the three distributions suggest that the pore size distribution does not have a significant influence on resistivity. However, we do find that for the symmetrical (rectangular and normal) distributions, the resistivity index is lower during imbibition for all saturations whereas for the unsymmetrical (lognormal) distribution, the resistivity index is lower during imbibition only toward residual oil saturation.

A possible explanation for such resistivity behavior may be the differences in the pore accessibility during drainage and imbibition in the networks with symmetrical and unsymmetrical pore size distributions. In a water-wet system, the pore accessibility is controlled by the smaller pores during drainage and the larger pores during imbibition. The two types of distributions possess different frequencies of smaller and larger pores and therefore, different pore accessibility during drainage and imbibition. This results in the differences in the form of hysteresis in the two distributions described above.

Standard deviation of pore size distribution.—To study the effects of standard deviation on the resistivity behavior, the modeling was repeated for the three pore size distributions with a higher value of standard deviation. These results are illustrated in Figures 3a, 3b, and 3c. Figure 3a contains the results for the rectangular distribution and standard deviation of 1.5 μm; Figure 3b contains the results for the normal distribution and standard deviation of 1.5 μm; and Figure 3c contains the results for the lognormal distribution and standard deviation of 2 μm.

The comparisons of Figures 3a, 3b, and 3c with Figures 2a, 2b, and 2c reveal a number of changes in the resistivity response as the standard deviation increases. The most noticeable is the reduction in the curvature of the resistivity plots. This is also reflected in a lowering of the two-point n values. These values are: 2.45 during drainage and 2.37 during imbibition for the rectangular distribution (Figure 3a); 2.22 during drainage and 2.20 during imbibition for the normal distribution (Figure 3b); and 2.01 during drainage and 2.38 during imbibition for the lognormal distribution (Figure 3c). As the standard deviation increases, the magnitude of hysteresis increases marginally; however, there is a large decrease in the value of the minimum water saturation at which electrical continuity is maintained across the network. The differences in the form of hysteresis between networks with symmetrical and unsymmetrical distributions, discussed in the previous section, persist at the higher standard deviation values.

The lower n values in the networks with higher standard deviation can be attributed to the fact that at any given water saturation, a water-wet network with a higher standard deviation of the pore size distribution has a larger number of pores filled with water resulting in improved electrical connectivity across the network. This is because at any given level of water saturation, the number of smaller pores (filled with water) with respect to the number of larger pores (filled with water) is always higher in the distributions with higher standard deviation.

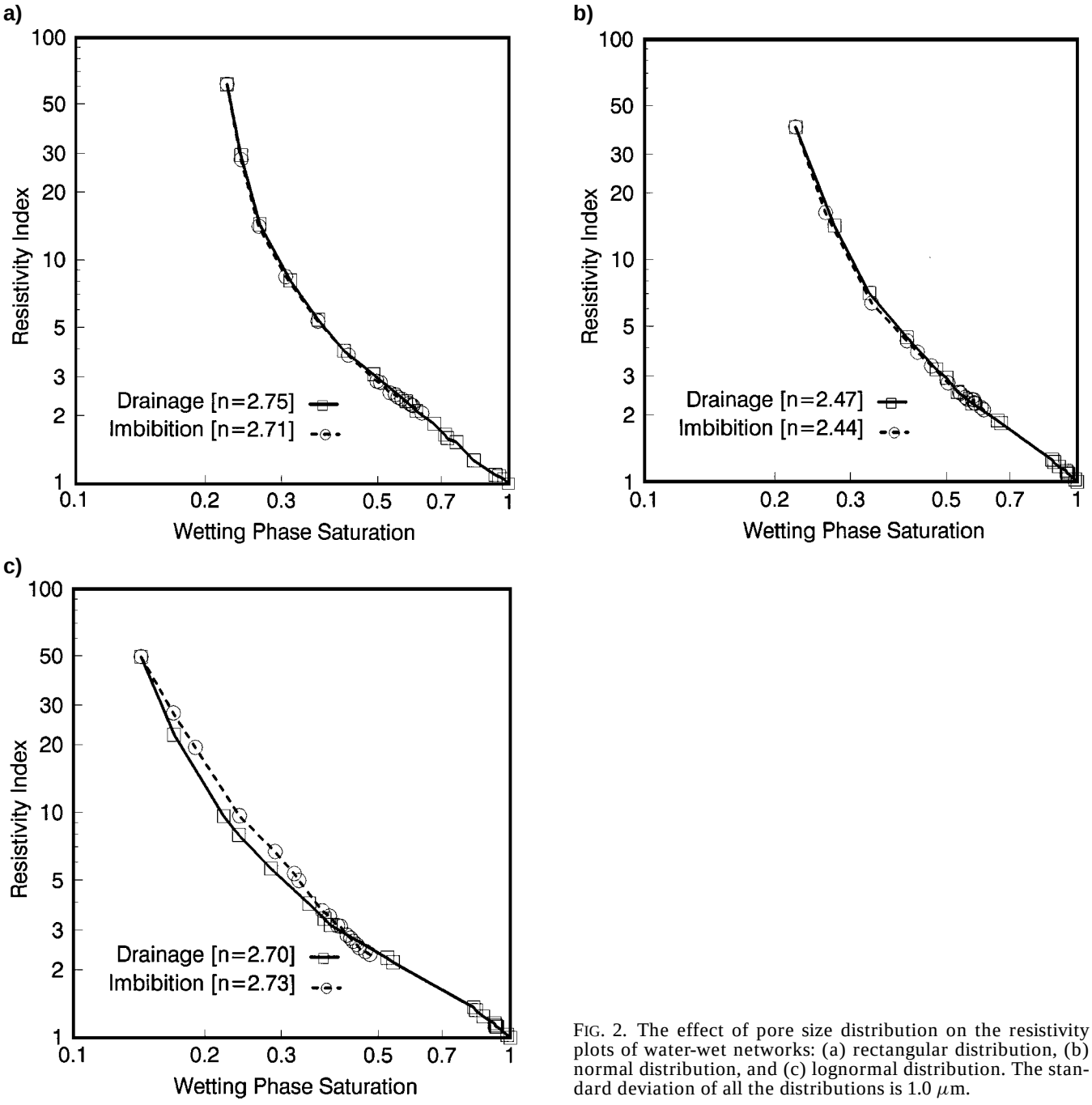

FIG. 2. The effect of pore size distribution on the resistivity plots of water-wet networks: (a) rectangular distribution, (b) normal distribution, and (c) lognormal distribution. The standard deviation of all the distributions is 1.0 μm.

This improved electrical connectivity translates into reduced n values and also in a lower value of the minimum water saturation at which electrical flow is possible across the network.

Pore size correlations.—The presence of positive correlation between the sizes of the neighboring pores in the water-wet networks is found to reduce hysteresis significantly. This can be seen by comparing Figure 4 with Figure 3c. Figure 4 shows the resistivity data for a positively correlated water-wet network with lognormal pore size distribution and a standard deviation of 2 μm. Figure 3c shows the resistivity plots for a similar but random network. The two-point n values for the correlated network are 1.79 during drainage and 1.96 during imbibition. Another noticeable effect of the pore size correlations is the reduction in the value of the minimum water saturation at which electrical conduction is possible across the network.

The presence of hysteresis in resistivity data, obtained with the present network model, is caused by the differences in the pore scale fluid distributions during drainage and imbibition. As explained earlier, for water-wet systems, the sequence of fluid displacements is controlled by the smaller pores during drainage and the larger pores during imbibition. In a positively correlated network, the pores of similar size tend to cluster together and therefore the network behaves as a set of connected subnetworks characterized by different pore size distributions. This reduces the control of the smaller pores during drainage

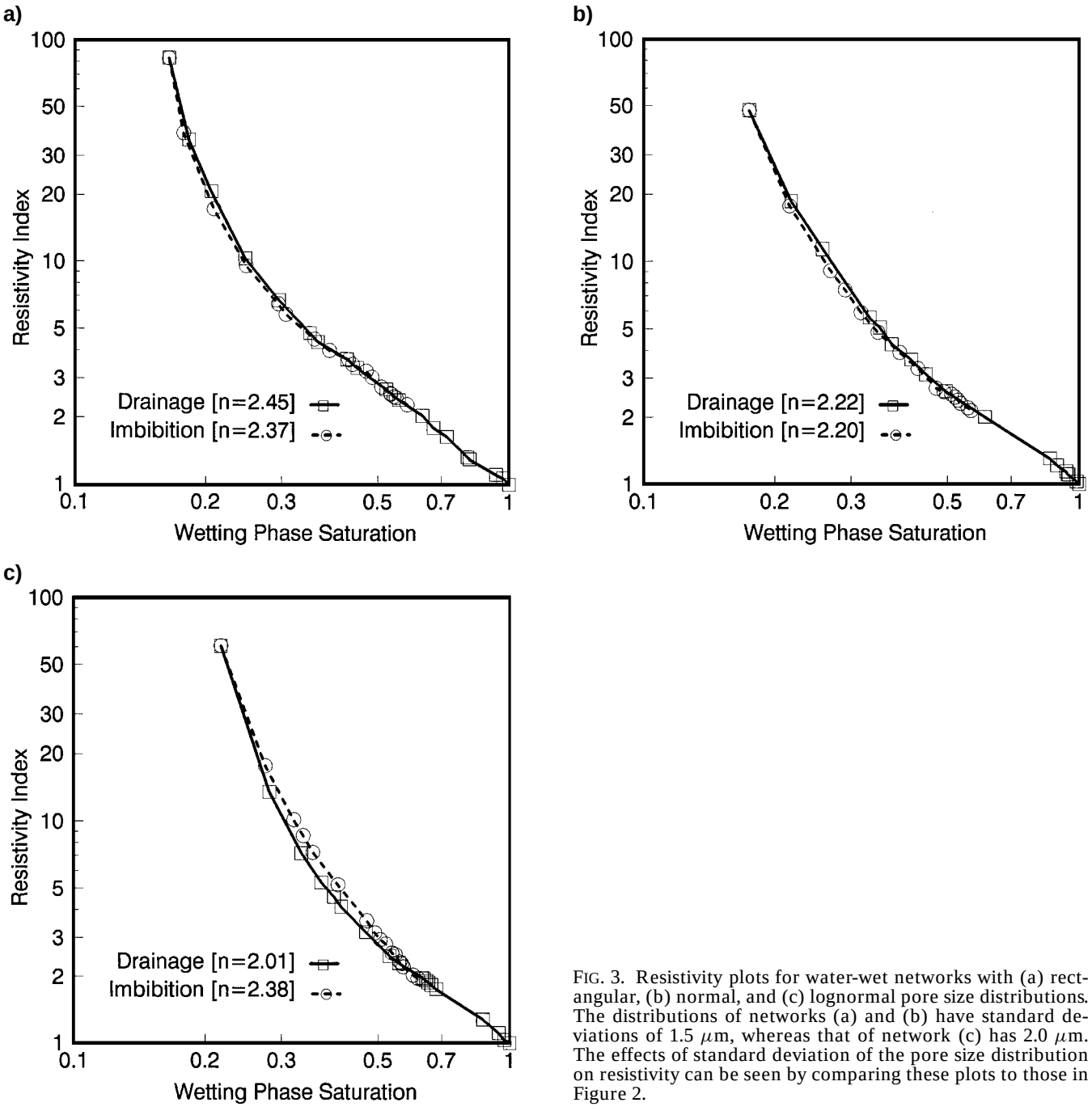

FIG. 3. Resistivity plots for water-wet networks with (a) rectangular, (b) normal, and (c) lognormal pore size distributions. The distributions of networks (a) and (b) have standard deviations of 1.5 μm, whereas that of network (c) has 2.0 μm. The effects of standard deviation of the pore size distribution on resistivity can be seen by comparing these plots to those in Figure 2.

and of larger pores during imbibition. The result is a reduction in the observed hysteresis. The enhanced pore accessibility in correlated networks also results in a lower value of the minimum water saturation at which electrical flow is possible across the network.

Effects of wettability

In the previous section, we determined the effects of pore structure on the resistivity behavior of water-wet networks. The assumption of water-wettability only dictated the distribution of the fluids inside the pore space; however, no surface water film was assumed to be present. In this section, we assess the effects of wettability by considering two end-member states for our network. The network is assumed to be either fully water-wet, in which case water preferentially fills the small pores and coats the solid surface, or fully oil-wet, in which case oil occupies the small pores and coats the solid surface.

The water film in the water-wet case is allowed to conduct electrical current thereby making additional paths available for electrical flow across the network. The electrical flow inside the water film is calculated using Ohm's law where the resistivity of the water is the same as the bulk water. Other mechanisms of electrical conduction such as electrical double layers are not considered. Our objective is not to calculate the exact magnitude of current through thin wetting films in water-wet rocks but to understand the role of surface water versus the bulk water in facilitating electrical conduction through a rock.

Effects of a thin wetting film in water-wet systems.—Figures 5a and 5b illustrate the influence of a wetting film on the resistivity behavior during drainage and imbibition. We consider three film thicknesses: 0, 1.0^{-8}, and 1.0^{-7} m. These are equivalent to 0%, 0.37%, and 3.70% of the mean pore radius of the network. As is obvious from these figures, the wetting film has a dramatic effect on the resistivity behavior of the network. In the presence of the film, the curvature in the resistivity plots is reduced substantially during both drainage and imbibition. Beyond a certain thickness, a linear relationship between $\log(I)$ and $\log(S_w)$ is obtained. A change in resistivity

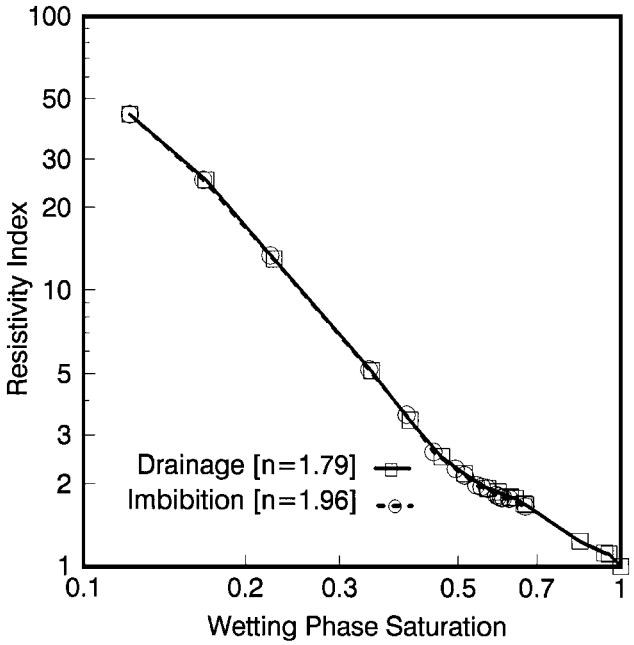

FIG. 4. Resistivity plots for a positively correlated water-wet network. The network has lognormal pore size distribution with a standard deviation of 2.0 μm. The effect of pore size correlation on the resistivity can be seen by comparing these plots with those in Figure 3c.

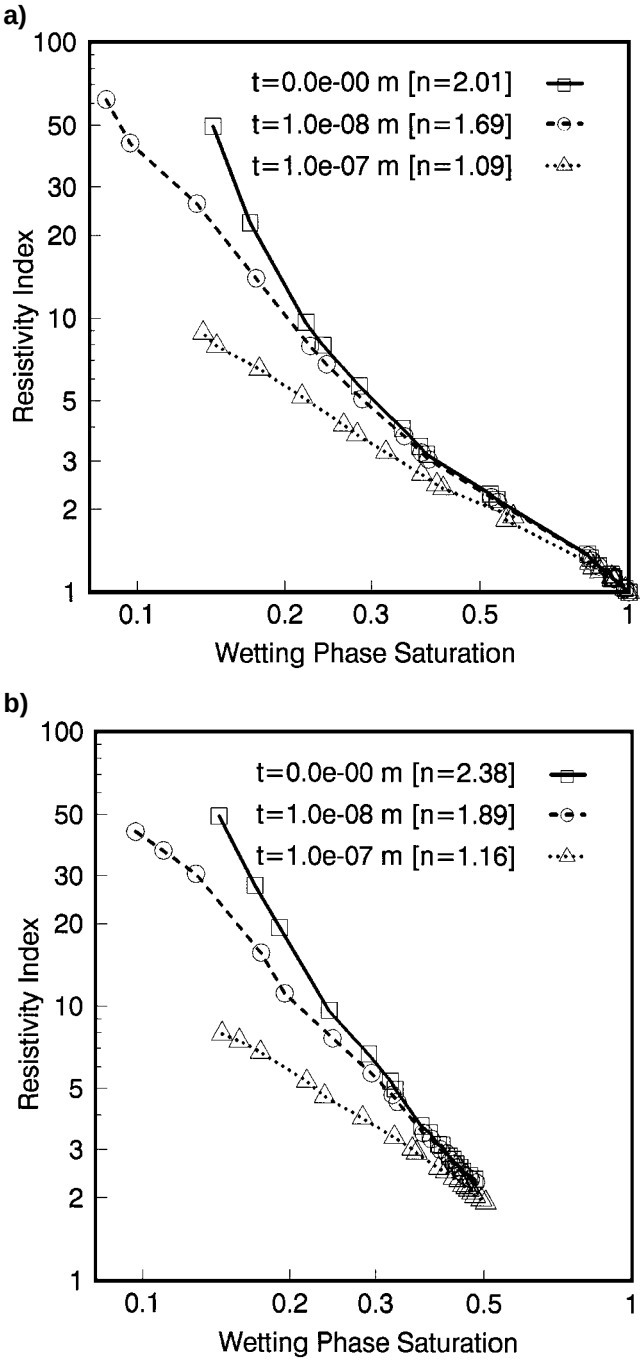

FIG. 5. The effect of thin wetting film on the resistivity of a water-wet network during (a) drainage, and (b) imbibition. The network has lognormal pore size distribution with a standard deviation of 2.0 μm. The symbol t in these figures represents the thickness of the film.

behavior is also apparent from the decrease in the two-point *n* values as the film thickness increases. These values are: 2.01, 1.69, and 1.09 during drainage and 2.37, 1.89, and 1.16 during imbibition for film thicknesses of 0, 1.0^{-8}, and 1.0^{-7} m. A comparison of the *n* values during drainage and imbibition indicates an increasing reduction in the hysteresis as the film thickness increases.

In a linear case (where the log-log plots of resistivity index and water saturation are linear) the resistivity increases at any given saturation is because of the removal of water from the network. In a nonlinear case (where the log-log plots of resistivity index and water saturation show an increase in slope as saturation decreases, e.g., different cases in Figures 2 and 3) the resistivity increase is caused partly by water being expelled from the network and partly by water inside the network becoming physically isolated from the electrically connected water. Here, the electrically connected water is the water inside the network that is electrically continuous from the upstream face to the downstream face of the network. The isolated water does not participate in the electrical conduction resulting in an additional increase in network resistivity in the nonlinear case. Since the proportion of the isolated water increases as the total water saturation inside the network decreases, the resistivity increases more with decreasing saturation at the lower saturations.

When a wetting film is present, it provides additional paths for electrical flow through the pores that are filled with oil and therefore at any given saturation, all the water inside the network is connected electrically. This results in a lower resistivity of the network and correspondingly in reduced *n* values and hysteresis. The magnitude of current through the water film itself is very small as compared to the current through the pore when it is filled completely with water. However, by providing critical electrical continuity toward low-water saturation, the presence of the water film drastically changes the overall resistivity behavior of the system.

The importance of electrical continuity of the conducting phase inside the network is demonstrated further by comparing Figures 6a and 6b to Figures 2c and 3c, respectively. In Figures 6a and 6b, the resistivity index is plotted as a function of the electrically continuous water saturation inside the network instead of the total water saturation as is the case in Figures 2c and 3c. All the networks are without a wetting film. The curvature in the resistivity plots is reduced significantly when electrically continuous water saturation is considered instead of the total water saturation. This is also apparent from the reduced *n* values. These results suggest that a network will have a tendency to display linear resistivity behavior (i.e., Archie-type response) when all the water inside the network participates in the electrical conduction across the network.

Oil-wet networks.—For oil-wet systems, we only consider normal and lognormal pore size distributions. This is because for water-wet systems, we did not find any significant differences between the resistivity responses of networks with rectangular and normal distributions. Also, for oil-wet systems, we do not expect to find any major differences between these two distributions.

The effects of wettability can be seen by comparing Figures 7a and 7b to Figures 2b and 2c, respectively. Figures 7a and 7b show the resistivity plots for oil-wet networks with normal and lognormal pore size distributions, respectively, each having a standard deviation of 1 μm. Figures 2b and 2c show the results for the corresponding water-wet networks. It is evident from this comparison that the resistivity behavior of an oil-wet system is very different from that of a water-wet system. This is consistent with many of the laboratory investigations cited earlier.

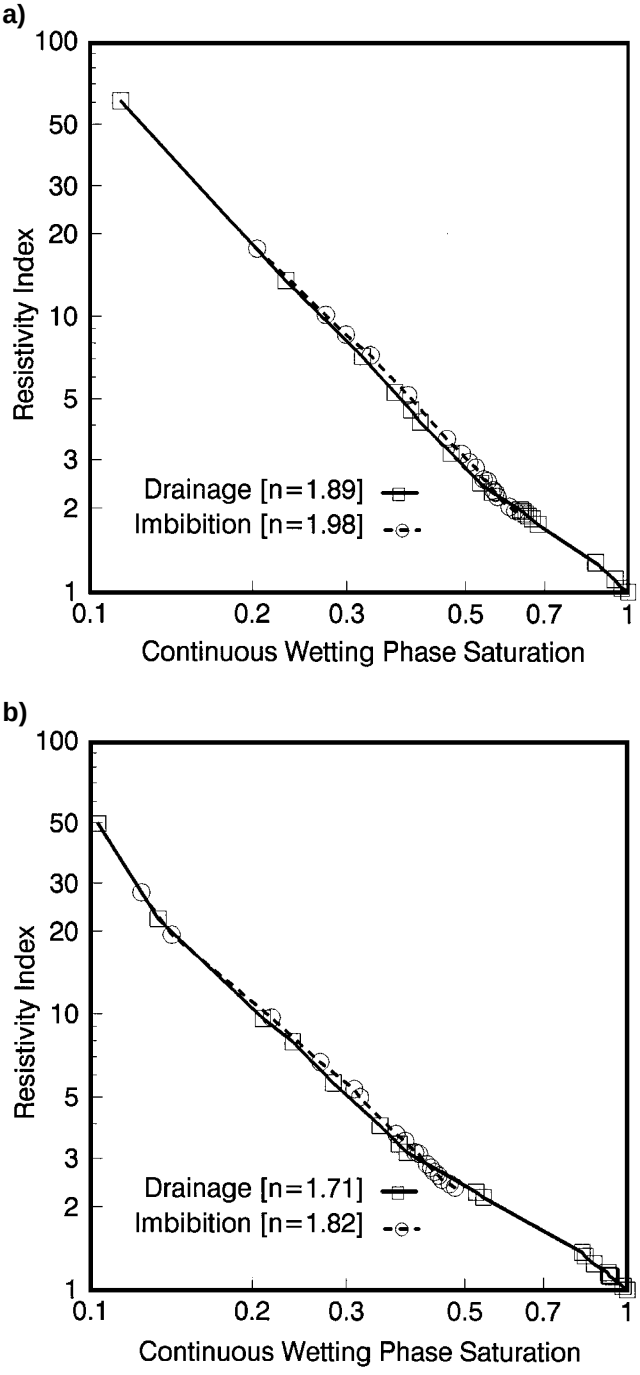

FIG. 6. The resistivity index of a water-wet network plotted as a function of continuous wetting phase saturation as opposed to the total wetting phase saturation. The network has a standard deviation of (a) 1.0 μm, and (b) 2.0 μm.

The oil-wet systems, unlike the water-wet systems, are characterized by high-resistivity index values during both drainage and imbibition. Also, the two-point *n* values for the oil-wet networks are significantly higher than those for the water-wet networks. For example, the two-point *n* values for the oil-wet network of Figure 7a are 3.60 during drainage and 5.86 during imbibition, whereas the *n* values for the corresponding water-wet network of Figure 2b are 2.47 during drainage and 2.44 during imbibition. Similarly, the *n* values for the oil-wet network of Figure 7b are 3.74 during drainage and 6.06 during imbibition, whereas for the corresponding water-wet network of Figure 2c, the *n* values are 2.70 during drainage and 2.73 during imbibition.

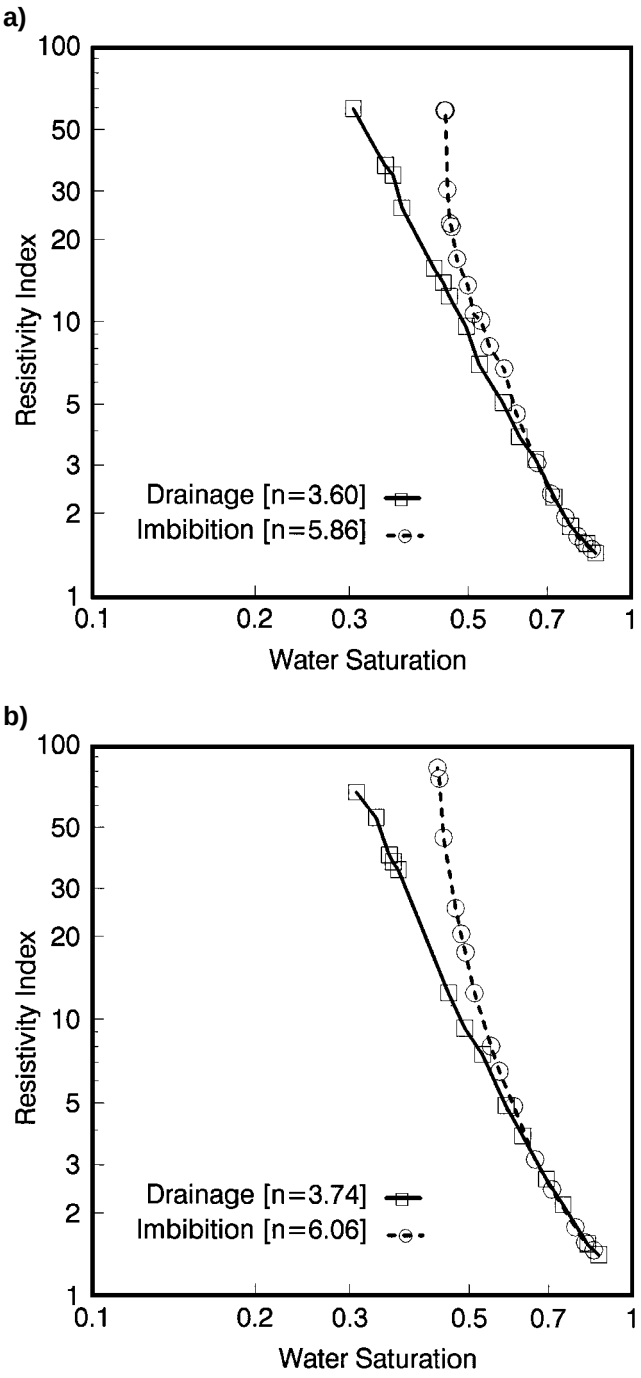

FIG. 7. Resistivity plots for an oil-wet network with (a) normal and (b) lognormal pore size distributions. Both cases have a standard deviation of 1.0 μm. The effects of wettability can be seen by comparing these plots to those in Figures 2b and 2c.

A comparison of the results for the two wettability cases also reveals a major difference in the magnitude of hysteresis in resistivity. The oil-wet systems, in contrast to the water-wet systems, display substantial hysteresis in resistivity. In addition, the hysteresis in the oil-wet systems increases as the level of water saturation decreases. In the water-wet systems the hysteresis is fairly independent of the water saturation. The form of the hysteresis is also different in the two systems. In the oil-wet systems, the resistivity index is consistently higher during imbibition for both types of pore size distributions. In the water-wet systems, the resistivity index is lower during imbibition for symmetrical (rectangular and normal) pore size distributions and higher during imbibition for networks with unsymmetrical (lognormal) distribution, except toward residual oil saturation.

The effects of pore structure on resistivity seem to be slightly more pronounced in the oil-wet systems than in the water-wet systems, although their magnitude is considerably lower than the effects associated with the changes in wettability discussed above.

A comparison of Figures 7a and 7b, which show the resistivity data for normal and lognormal distributions, each with a standard deviation of 1 μm, suggests that the pore size distribution has a negligible influence on the resistivity of oil-wet networks. This is similar to what we observed for the water-wet networks.

The effects of standard deviation on the resistivity of the oil-wet case can be seen by comparing the data of Figures 7a and 7b with those of Figures 8a and 8b, respectively. Figures 8a and 8b show the resistivity plots for the normal pore size distribution with a standard deviation of 1.5 μm and the lognormal distribution with a standard deviation of 2.0 μm, respectively. The rate of increase of resistivity index during drainage, as the water saturation decreases, is lower for networks with higher standard deviation. However, the rate of increase of resistivity index during imbibition, as the water saturation decreases, is higher for networks with higher standard deviation. The two-point *n* values for the two standard deviations display this same trend. For example, the *n* values for the normal distribution during drainage are 3.60 (Figure 7a) and 3.41 (Figure 8a) for standard deviations of 1 μm and 1.5 μm, respectively; while the *n* values for normal distribution during imbibition are 5.86 (Figure 7a) and 6.52 (Figure 8a) for standard deviations of 1 μm and 1.5 μm. Similarly, the *n* values for the lognormal distribution during drainage are 3.74 (Figure 7b) and 3.24 (Figure 8b) for standard deviations of 1 μm and 2 μm, respectively; while the *n* values for lognormal distribution during imbibition are 6.06 (Figure 7b) and 8.17 (Figure 8a) for standard deviations of 1 μm and 2 μm, respectively.

The effects of standard deviation on the resistivity response of the oil-wet networks, described above, can be attributed to the number of pores filled with water at any given water saturation. During the initial stages of drainage, water displaces oil from the larger pores. As the standard deviation increases, the pore size distribution becomes wider and the size of the larger pores also increases. Therefore, corresponding to a given

increase in the water saturation, fewer pores are filled with water. As a consequence of this, the decrease in resistivity is smaller resulting in lower n values. During the imbibition cycle, oil displaces water from the smaller pores. As the standard deviation increases, the frequency of smaller pores with respect to the larger pores increases. Therefore, corresponding to a given decrease in the water saturation, water is displaced from a relatively larger number of pores, and, therefore, the increase in the resistivity is larger resulting in higher n values.

The effect of positive pore size correlation on the resistivity of oil-wet networks can be seen by comparing Figure 9 with Figure 8b. Figure 9 shows the resistivity data for a positively correlated oil-wet network with lognormal pore size distribution and a standard deviation of 2 μm. Figure 8b shows the resistivity plots for a similar but random network. As is evident from this comparison, the hysteresis in resistivity is almost eliminated when the pore sizes of an oil-wet network are correlated positively. These results are similar to those for the water-wet case depicted in Figure 4. The resistivity of the correlated network during both drainage and imbibition is characterized by lower two-point n values (2.67 during drainage and 2.75 during imbibition) in contrast to the resistivity of a similar random network (Figure 8b with n values of 3.24 during drainage and 8.17 during imbibition).

As explained earlier for the water-wet systems, pores of similar sizes tend to cluster together in a positively correlated network. This reduces the control of the smaller pores on the sequence of fluid displacements during drainage and that of larger pores during imbibition. The result is reduction in the observed hysteresis.

The differences in the resistivity behaviors of the water-wet and oil-wet networks are caused by different pore scale distributions of the conducting phase in the two cases. In a water-wet network, the oil occupies the larger pores and the water remains in the smaller pores. The situation is reversed completely in the oil-wet system where the water occupies the larger pores and the oil occupies the smaller pores. Since oil occupies the larger pores in the water-wet system, a given volume of oil

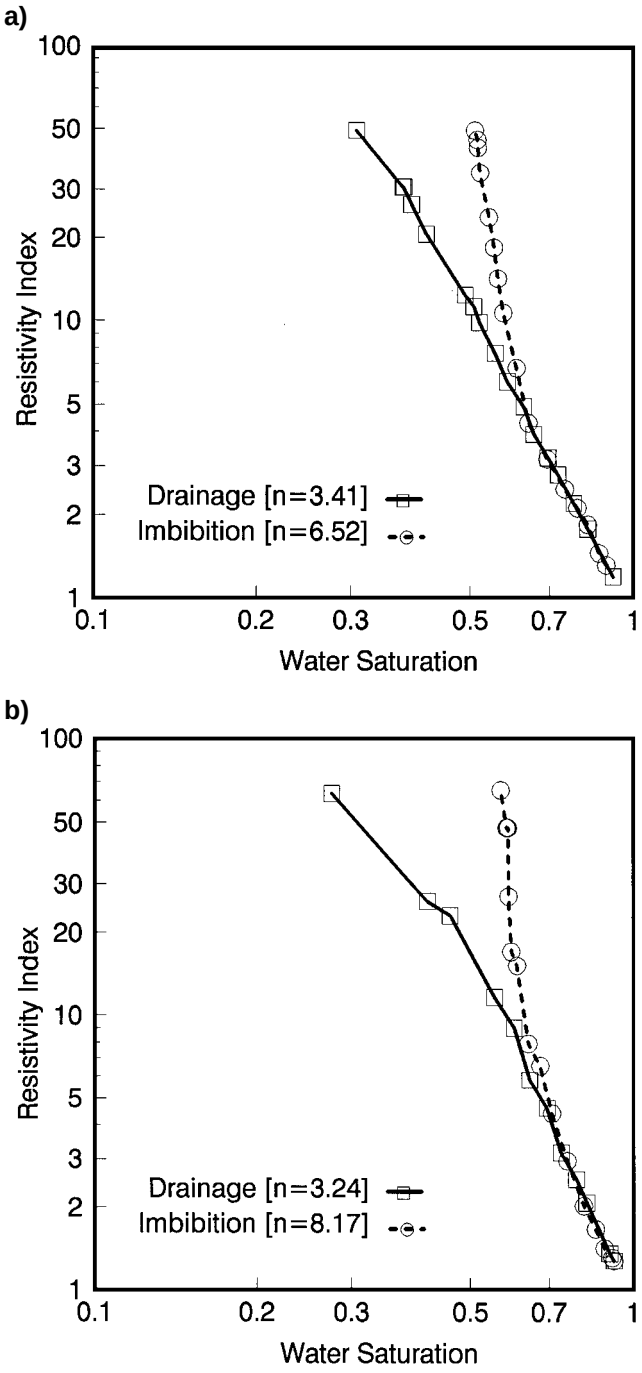

FIG. 8. Resistivity plots for an oil-wet network with (a) normal pore size distribution with a standard deviation of 1.5 μm, and (b) lognormal pore size distribution with a standard deviation of 2.0 μm. The effects of increasing the standard deviation in oil-wet networks can be seen by comparing these plots to those in Figure 7.

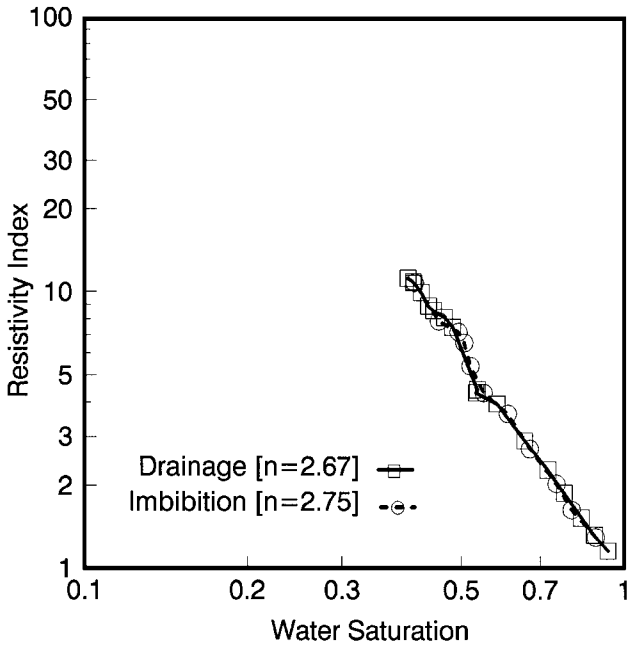

FIG. 9. Resistivity plots for a positively correlated oil-wet network. The network has lognormal pore size distribution with a standard deviation of 2.0 μm. The effect of pore size correlation on the resistivity of an oil-wet network can be seen by comparing these plots with those in Figure 8b.

when injected into the network displaces water from a smaller number of pores than it would in the case of an oil-wet network. Therefore, at any given water saturation the number of pores filled with water is always higher in the water-wet network resulting in increased connectivity between different pockets of water inside the network. Because of this increased connectivity, at any given water saturation, the amount of isolated water in a water-wet network is smaller than that in a similar oil-wet network. Consequently, corresponding to a given decrease in the water saturation, the resistivity increase in an oil-wet network is greater than that in a water-wet network. This results in higher n values and greater hysteresis in oil-wet systems.

FURTHER DISCUSSION

The present work has important implications for the interpretation of resistivity logs for the prediction of in-situ water saturation. Some of these implications are discussed in this section.

In water-wet systems, the most important factor in determining the resistivity response is found to be the presence and thickness of a conducting surface water film. The results of this work suggest that Archie's law, which assumes a constant n value at all saturations, may be realized only in strongly water-wet systems in which a sufficiently thick surface water film is present. The film ensures the connectivity of isolated pockets of water inside the pore space which is essential for realizing an Archie type resistivity behavior. Since the proportion of the isolated water increases as the level of total water saturation decreases, the film is critical at low levels of water saturation. In the presence of the water film, the effects of saturation history, that is, hysteresis between drainage and imbibition cycles, are substantially reduced.

The sensitivity of resistivity to the thickness of the film in water-wet rocks has important consequences when fluids other than in-situ fluids are employed in tests on core plugs for reservoir characterization. For example, it is common practice to use gas and water to characterize the resistivity behavior of core samples originally saturated with oil and formation water. This practice can result in significant errors in the estimation of n values as noted by Longeron et al. (1989) who found n to be 1.26 for an air/brine combination and 1.65 for an oil/brine combination on the same core plug. This difference in resistivity is primarily caused by differences in the thickness of the water film in the two cases. As shown in Bretherton (1961), the thickness of the film on the walls of a cylindrical capillary during drainage depends on the viscosity of the displacing phase with respect to the viscosity of the wetting phase and the capillary pressure. When the viscosity of the displacing fluid is lower than that of the wetting phase, the water film is thicker resulting in lower n values. In general therefore, air displacing brine will yield lower n values than oil displacing brine.

Wettability is found to be the most important factor controlling the resistivity response of a partially saturated rock. The n values and the magnitude of hysteresis between drainage and imbibition cycles is higher substantially in the oil-wet systems. In addition, the hysteresis in oil-wet systems increases as the level of water saturation decreases whereas in water-wet systems, the magnitude of hysteresis is fairly independent of the water saturation. The strong dependence of resistivity response on the wettability demands that for reservoir characterization, electrical measurements be done on cores in which the in-situ wettability is preserved. If it is not possible to preserve the wettability of a core, the tests should be done on the cores in which the original wettability is restored.

Both water-wet and oil-wet networks show hysteresis in resistivity. However, the magnitude of hysteresis is significantly higher in the oil-wet systems. The presence of hysteresis has important implications in the interpretation of electric logs used for estimation of oil in the reservoirs. The n values used for the estimation of oil reserves must be based on the appropriate part of the electrical resistivity plots. For example, for initial oil estimates in water-wet reservoirs, the drainage curve would be more appropriate because this is the process that took place when oil was first emplaced. For other parts of the water-wet reservoir, such as the oil-water transition zones, the imbibition curve would be more appropriate. The imbibition curve would also be appropriate for the estimation of oil in water-wet reserves subject to water flooding.

In the presence of a positive correlation between the sizes of the neighboring pores of the network, the hysteresis is reduced significantly in both the water-wet and oil-wet systems. Natural porous media are found to possess varying degrees of pore size correlations. In their limestone sample, Wardlaw et al. (1987) found a very high degree of correlation between the sizes of the neighboring pores. However, in their sandstone sample, the degree of correlation was small. The pore size correlation is an important pore structure parameter, and resistivity measurements may provide a means for distinguishing correlated porous media from the random ones.

CONCLUSIONS

We have employed a 3-D network model of porous media to assess the effects of certain pore structure features and wettability on the resistivity index/water saturation relationship of partially saturated rocks. This investigation supports the following important conclusions:

1) Archie's law may be realized only in strongly water-wet systems in which a sufficiently thick water film is present.
2) In water-wet systems, the resistivity behavior is sensitive to the thickness of the surface water film. Therefore, laboratory n values should be determined with fluids representative of the reservoir fluids.
3) Wettability has a dominant influence on the resistivity index/water saturation relationship of partially saturated rocks. Oil-wet systems display substantially higher n values and significant hysteresis between drainage and imbibition cycles. Moreover, the saturation exponent itself can be a function of saturation. Therefore, for reservoir characterization, n values should be measured on cores with wettability and saturation representative of the reservoir.
4) Hysteresis must be taken into account when interpreting the resistivity well logs. This is particularly important when the reservoir under question is oil-wet.
5) The hysteresis in both the water-wet and oil-wet systems is reduced substantially when the pore sizes possess a positive correlation. The resistivity measurements may therefore provide a means of distinguishing correlated from uncorrelated porous media.

ACKNOWLEDGMENTS

This research was supported primarily by funding to R. Knight from Conoco, Imperial Oil, Petro-Canada, Shell Canada, and an Industrially Oriented Research Grant from the Natural Sciences and Engineering Research Council of Canada (NSERC). Additional funding was obtained from an NSERC Research Grant to R. Knight.

REFERENCES

Archie, G. E., 1942, The electrical resistivity log as an aid in determining some reservoir characteristics: Trans. AIME, **146**, 54–61.

Bretherton, F. P., 1961, The motion of length bubbles in tubes: J. Fluid Mechanics, **10**, 166–171.

Chatzis, I., and Dullien, F. A. L., 1985, The modeling of mercury porosimetry and the relative permeability of mercury in sandstones using percolation theory: Int. Chem. Eng., **25**, 47–66.

Donaldson, E. C., and Bizerra, M. J., 1985, Relationship of wettability to saturation exponent: Third International UNITAR/UNDP Heavy Crude and Tar Sands Conference, preprints **2**: United Nations Institute for Training and Research, Information Center for Heavy Crude and Tars, 664–684.

Donaldson, E. C., and Siddiqui, T. K., 1989, Relation between Archie saturation exponent and wettability: Soc. Petr. Eng., Formation evaluation, 359–362.

Fatt, I., 1956, The network model of porous media III: Trans. AIME, **207**, 144–181.

Greenberg, R. J., and Brace, W. F., 1969, Archie's law for rocks modeled by simple networks: J. Geophys. Res., **74**, 2099–2102.

Keller, G. V., 1953, Effect of wettability on the electrical resistivity of sand: Oil and Gas J., **51**, No. 34, 62–65.

Lewis, M. G., 1988, The effects of stress and wettability on electrical properties of rocks: M.Sc. Eng. thesis, University of Texas at Austin.

Longeron, D. G., Argaud, M. J., and Feraud, J.-P., 1989, Effect of overburden pressure and the nature of microscopic distribution of fluids on electrical properties of rock samples: Soc. Petr. Eng., Formation evaluation, June, 194–202.

Morgan, W. B., and Pirson, S. J., 1964, The effect of fractional wettability on the Archie saturation exponent: Trans. 5th Ann. Symp. Soc. Prof. Well Log. Analysts, Section B., 1–13.

Mungan, N., and Moore, E. J., 1968, Certain wettability effects on electrical resistivity in porous media: J. Can. Petr. Tech., **7**, No. 1, 20–25.

Nicholson, D., Petrou, J. K., and Petropolous, J. H., 1988, Relation between macroscopic conductance and microscopic structural parameters of stochastic networks with application to fluid transport in porous materials: Chem. Eng. Sci., **43**, 1385–1393.

Rust, C. F., 1957, A laboratory study of wettability effects on electrical resistivity in porous media: Soc. Petr. Eng., Paper **986-G**, 1–16.

Sanyal, S. K., and Ramey, H. K., Jr., 1973, Effect of temperature on the electrical resistivity of porous media: The Log Analyst, **14**, No. 2, 10–14.

Shankland, T. J., and Waff, H. S., 1974, Conductivity in fluid bearing rocks: J. Geophys. Res., **79**, 4863–4868.

Sharma, M. M., Garrouch, A., and Dunlop, H. F., 1991, Effects of wettability, pore geometry and stress on electrical conduction in fluid saturated rocks: The Log Analyst, **32**, 511–526.

Swanson, B. F., 1980, Rationalizing the influence of crude wetting on the reservoir fluid flow with electrical resistivity behavior: J. Petr. Tech., August, 1459–1464.

Sweeney, S. A., Jennings, H. V., 1960, The electrical resistivity of preferentially water-wet and preferentially oil-wet carbonate rocks: Producers Monthly, **24**, No. 7, 29–32.

Tsakiroglou, C. D., and Payatakes, A. C., 1991, Effects of pore-size correlations on mercury porosimetry curves: J. Colloid and Interface Science, **146**, 479–494.

Wang, Y., and Sharma, M. M., 1988, A network model for the resistivity behavior of partially saturated rocks: Trans. 29th Ann. Logging Symp.: Soc. Prof. Well Log. Analysts.

Wardlaw, N. C., Li, Y., and Forbes, D., 1987, Pore-throat size correlations from capillary pressure curves: Transport in porous media, **2**, 597–614.

Wei, J. Z., and Lile, O. B., 1991, Influence of wettability on two- and four-electrode resistivity measurements on Berea sandstone plugs: Soc. Petr. Eng., Formation evaluation, 470–476.